Engineering and Technology Journal e-ISSN: 2456-3358

Volume 11 Issue 01 January-2026, Page No.-8538-8553

DOI: 10.47191/etj/v11i01.14, I.F. – 8.482

Adsorption of Arsenic from Mine-Wastewater Using Iron Impregnated Activated Carbon: Effect of Operating Parameters and Kinetic Modelling

Mark Dave Verdejo[1], Djoan Kate Tungpalan[2], Candy Mercado[3]

[1]Master of Science in Environmental Engineering Student, University of the Philippines, Diliman.

[2]Department of Mining, Metallurgical, and Materials Engineering, College of Engineering, University of the Philippines, Diliman.

[3]Department of Mining, Metallurgical, and Materials Engineering, College of Engineering, University of the Philippines, Diliman.

Highlights

- Iron-oxide impregnated activated carbon was prepared for arsenic removal.
- SEM-EDX confirmed iron impregnation via surface adsorption and pore filling.
- Modified activated carbon achieved up to 99% arsenic removal efficiency
- Adsorption followed pseudo-second order kinetic.
- Coexisting metal in mine-wastewater influenced arsenic adsorption rate

Graphical Abstract

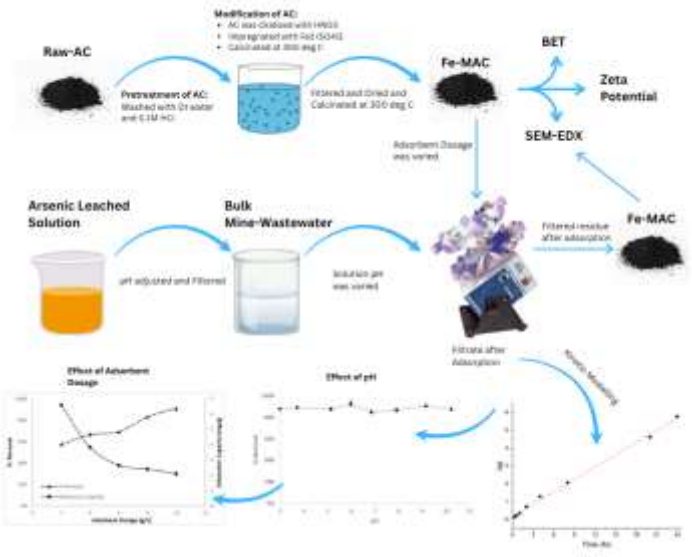

ABSTRACT: Activated carbon presents a promising alternative in arsenic treatment as it is low-cost and does not produce hazardous by-product. It has been proven to be effective in removing arsenic in wastewater, however, most of the studies were conducted using synthetic wastewater that does not necessarily represent the actual condition of a mine wastewater. The main objective of this study is to remove arsenic from mine-wastewater using iron-oxide impregnated activated carbon. Results showed that the iron was successfully impregnated to activated carbon through surface adsorption and pore filling based on SEM-EDX analysis. The modification enhances the affinity of the activated carbon to arsenic achieving maximum 99% arsenic removal. The adsorption of arsenic was not significantly affected by the initial pH due to convergence to near neutral final pH regardless of initial pH. And higher adsorbent dosage significantly increased the removal with maximum at 10 g/L adsorbent dosage. The adsorption data is well fitted on pseudo-second order suggesting that the rate-limiting step may involve chemisorption and intraparticle diffusion contributes to the adsorption process. And the presence of other metals affected the rate of adsorption of arsenic.

I. INTRODUCTION

The presence of arsenic in water and wastewater poses significant challenges worldwide because of its toxicity and frequency of human exposure (CDCP, 2024). it is also included in WHO's 10 chemicals of major public concern. Long term effects of arsenic include skin lesion (hyperkeratosis), skin cancer, diabetes, developmental effects, and cardiovascular disease. WHO, 2022 estimated that approximately 140 million people in 70 countries have been drinking water with arsenic above the maximum

permissible value of 10 µg/L. According to Podgorski & Berg (2020), the primary source of arsenic exposure is through the ingestion of contaminated groundwater, a critical concern reported in several countries such as Bangladesh, China, India, Myanmar, Taiwan, and Mexico (Ahmad et al., 2018; Liang et al., 2016; Phyu et al., 2020; Alarcón-Herrera et al., 2013). Arsenic can be released into the environment through natural processes like volcanic eruptions, rock weathering, other geochemical reactions, and anthropogenic activities. Anthropogenic sources of arsenic are mining, ore processing and smelting, industrial discharge, agricultural pesticides, and coal burning. Among these, ore processing, mining, and smelting are major sources of arsenic worldwide (Garelick et al., 2009) and arsenic contamination is mainly derived from arsenic-bearing mining residues (Zhuang et al., 2023).

Numerous treatment methods are available for the removal of arsenic in water including precipitation, ion exchange, electrochemical reduction, bioremediation, coagulation, and adsorption. However, each of them has its one or more drawbacks and limitations such as complexity of process, high cost of operation and maintenance, required pretreatment, sludge production, and production of toxic waste (Zakhar et al., 2018b) (Kobya et al., 2020). Among these methods adsorption is the most practical method to use because of its ease of operation, cost-effectiveness, no hazardous by-products, and high efficiency (Weerasundara et al., 2021) (Verma & Singh, 2019).

Iron impregnated activated carbon (AC) is one of the promising alternatives in removing arsenic because of its low cost, sustainability, and does not produce hazardous by-products (Siddiqui & Chaudhry, 2017a). AC is widely used to remove various pollutants due to its high surface area. However, raw AC is less effective in removing arsenic due to its negatively charge (Kalaruban et al., 2019, Arcibar-Orozco et al., 2014). This limitation is often addressed by introducing active agents onto the surface of activated carbon (AC), such as iron oxides, which enhance surface reactivity and thereby improve the adsorption capacity for arsenic (Zhang et al., 2007 and Sigrist et al., 2014). However, it is important to note that simply increasing the amount of iron oxides does not necessarily result in a proportional increase in arsenic adsorption capacity (Sigrist et al., 2014). Operational parameters such pH, adsorbent dosage, contact time, competing ions, and nature of iron salt play significant roles in arsenic removal. Since arsenic speciation is strongly dependent on pH, it is considered the most critical parameter influencing arsenic adsorption. The pH of the solution not only governs arsenic speciation but also affects the surface chemistry of the adsorbent, particularly when functional groups are present (Siddiqui & Chaudhry, 2017b). Apart from pH, when various ions compete for adsorption on the same adsorbent surface, this can influence both the adsorption capacity and the selectivity of the adsorbent. Specific adsorption of heavy metals in affinity sequence is related to ionic radius and electronegativity. For instance, Shan et al. (2020) reported that in multi-component adsorption containing Pb^{2+}, Cd^{2+}, Cu^{2+}, Ni^{2+}, and Zn^{2+}, the removal efficiency of each ion decreased compared to single-component systems due to competitive adsorption. With lead showing the smallest reduction in removal efficiency, indicating its superior competitiveness in adsorption. Similarly, Pawar et al. (2018) observed the removal trend in multi-component system follows the trend of Pb^{2+} > Cd^{2+} >As (V), this is attributed to the ionic radius and electronegativity of these metals. On the other hand, common anions such as bicarbonate, sulfate, and phosphate exert minimal influence on the removal of both As(III) and As(V) (Wang et al., 2022). Similarly, the presence of competing ions including potassium carbonate (K_2CO_3), magnesium sulfate ($MgSO_4$), sodium nitrate ($NaNO_3$), and calcium chloride ($CaCl_2$) was found to have little to no effect

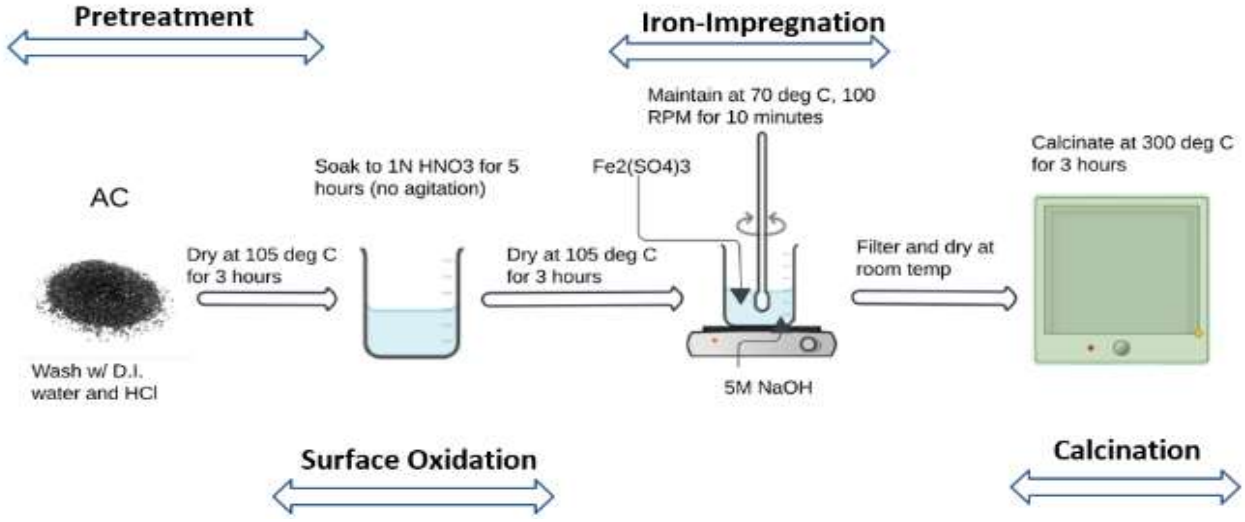

Figure 1:Modification of Activated Carbon (modified from Zhang et al., 2007)

on the adsorption of As(V) (Karmacharya et al., 2016).

Iron impregnated activated carbon is well established to be effective in removing arsenic from water. However, previous studies are usually explored using synthetic wastewater, which do not represent an actual wastewater. The novelty of this study is the application of iron-impregnated active ted carbon for the removal of arsenic from actual mine wastewater, thereby providing a more realistic assessment of its performance under practical conditions.

2. MATERIALS AND METHOD

2.1 Materials

Commercial powdered activated carbon was used in this study. The arsenic contaminated mine wastewater is from the product of a neutralized-wastewater from leaching of an arsenic-bearing copper ore.

2.2 Modification of Activated Carbon

The modification was done by first applying surface oxidation using 1N nitric acid for 5 hours at room temperature without agitation to modify its surface property. Then, it was mixed to a solution of $Fe_2(SO_4)_3$ and 5M of NaOH for 10 minutes at 70 °C, 100 rpm, and pH 10.5, modified from (Zhang et al., 2007). The solution was then filtered and washed with DI water until no iron was detected on the filtrate. Finally, the AC was calcinated at 300 °C for 3 hours. The iron-impregnated activated carbon is referred to as Fe-MAC (Figure 1).

2.3 Batch Adsorption Experiment

Adsorption experiments were carried out in end-over end shaker at constant agitation of 80 rpm and at ambient temperature for 24 hours. The pH of the mine wastewater was varied to determine its influence on the adsorption of arsenic. Different adsorbent dosages were also investigated. All experiments were carried out in duplicates (Figure 2). The treated mine-wastewater was analyzed in the ICP-OES for arsenic, copper, nickel and iron, along with other elements.

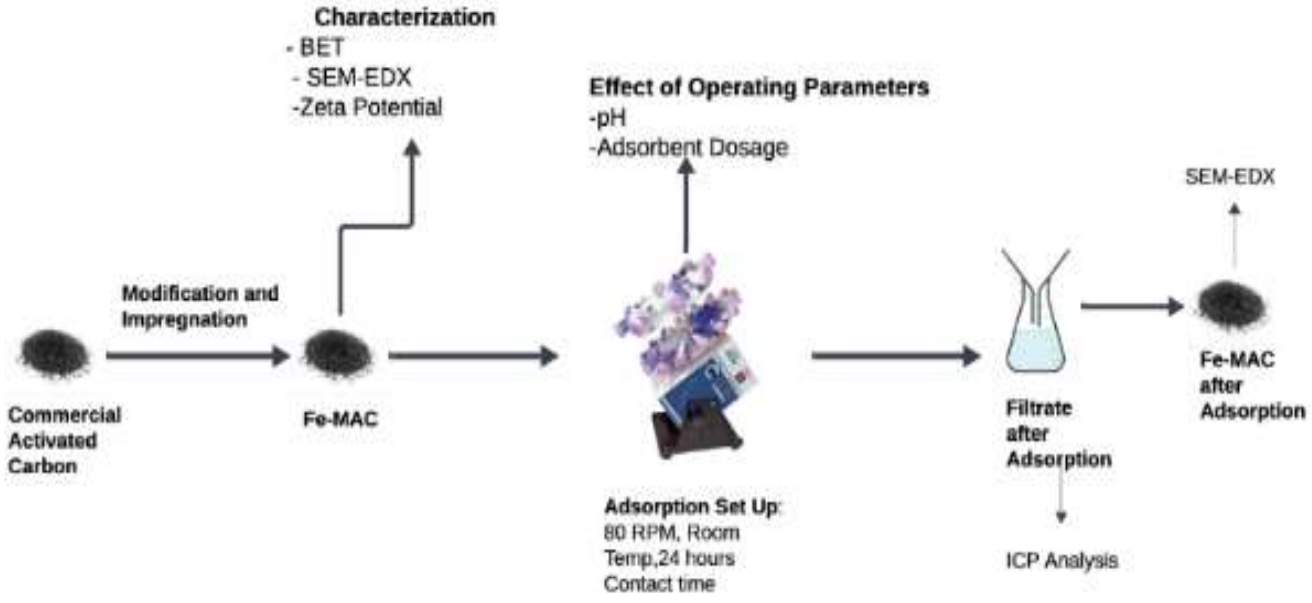

Figure 2: Summary of Methodology

3. RESULTS AND DISCUSSION

3.1 Characterization of Mine-Wastewater

The multi-element ICP analysis revealed that the mine-wastewater contains high concentration of arsenic and other metals such as nickel and copper. The major elements present in the mine-wastewater is presented in Table 1

Table 1: Elemental Concentration of Mine-Wastewater

Parameter	Value	Unit	Parameter	Value
As	149.41	ppm	pH	≈7
Al	17.45	ppm	Odor	Rotten Egg
Fe	15.26	ppm	Color	Yellowish brown
Ni	3.72	ppm		
Cu	3.92	ppm		

3.2 Characterization of Activated Carbon

3.2.1 Morphology and Elemental Mapping

Element	Atomic %
C	76.1
O	16.7
Al	6.4
Si	0.3
S	0.2
Ti	0
Fe	0.2

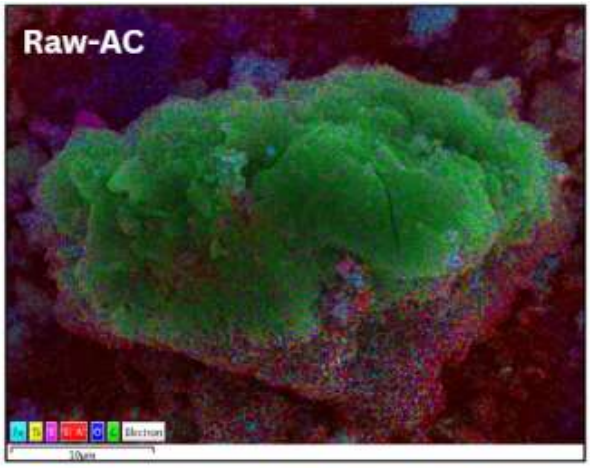

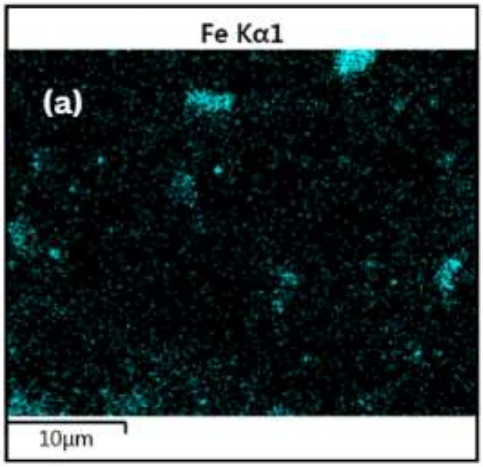

Element	Atomic %
C	88.54
O	10.22
Al	0.41
Si	0.26
S	0.13
K	0.02
Ca	0.01
V	0.01
Fe	0.37

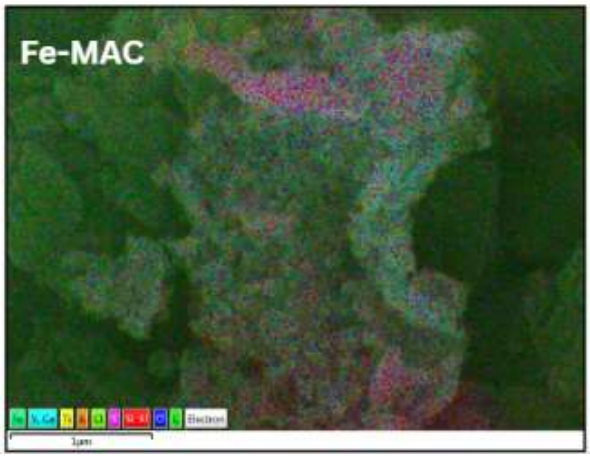

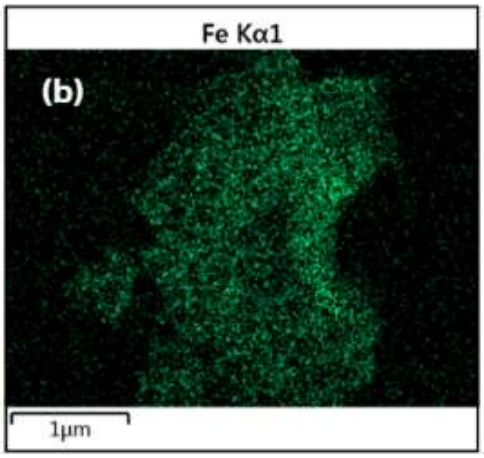

Figure 3: Elemental Mapping and Composition of Activated Carbon Before and After the Modification

The raw-AC contains 76.1% carbon confirming that the material is predominantly carbonaceous and 16.7% oxygen indicating a presence of oxygen containing functional groups. Iron was also detected in the raw AC suggesting that the carbon contains trace level of iron (Figure 3). To confirm the attachment of iron on AC after the impregnation, SEM-EDX analyses were conducted. Figure 3 showed that changes were observed on the atomic percent concentration of the elements before and after the impregnation. The iron content increased from 0.2% to 0.37% confirming the impregnation of iron. The increase in carbon content from 76.1 % to 88.5% suggests the successful removal of non-carbon impurities, as evidenced by the decrease in aluminum content from 6.4 % to 0.4% and oxygen content from 16.7 % to 10.2% after the modification. This to the decrease can be due to the decrease of oxide from the aluminum oxide.

To determine the homogeneity of iron impregnation, other spectra with smaller coverage and brighter reflection of particles were picked, as brighter appearance in the SEM image means higher atomic number (Waseem, 2023). The atomic numbers of C, Al, Si, and Fe are 6, 13, 14, and 26 respectively, thus the lighter appearance of spectrum 7 compared to 6 was due to the increase of concentrations of these elements including iron as shown Figure 5. The results indicate that the impregnated iron is unevenly distributed among the particles, suggesting non-homogeneous dispersion. This could be due to several reasons, such as insufficient impregnation time of only 10 minutes, low agitation speed (100 rpm) during impregnation, as evidenced by observed particle settling, and the variability of surface properties of the Raw-AC such pore sizes, porosity, and particle size as observed in the SEM image. On the other hand, the SEM EDX analysis of a randomly picked particle of Fe-MAC showed homogenous distribution of iron within particle. Nonetheless, the SEM EDX analysis of a randomly picked activated carbon particle of Fe-MAC showed homogenous distribution of iron within the particle (Figure 3b).

Changes in surface morphology of the Fe-MAC as seen in the SEM image confirmed the attachment and pore filling of iron after the impregnation. In Figure 4 (b and d), it can be observed that multiple spherical particles are attached to and deposited on the surface and within the pores of Fe-MAC that is not present on the Raw-AC (Figure 4 -a and c). These spherical particles could be the iron. The measured particle size of suspected iron deposits is within the range of 4-65 nm with mean of 31 nm.

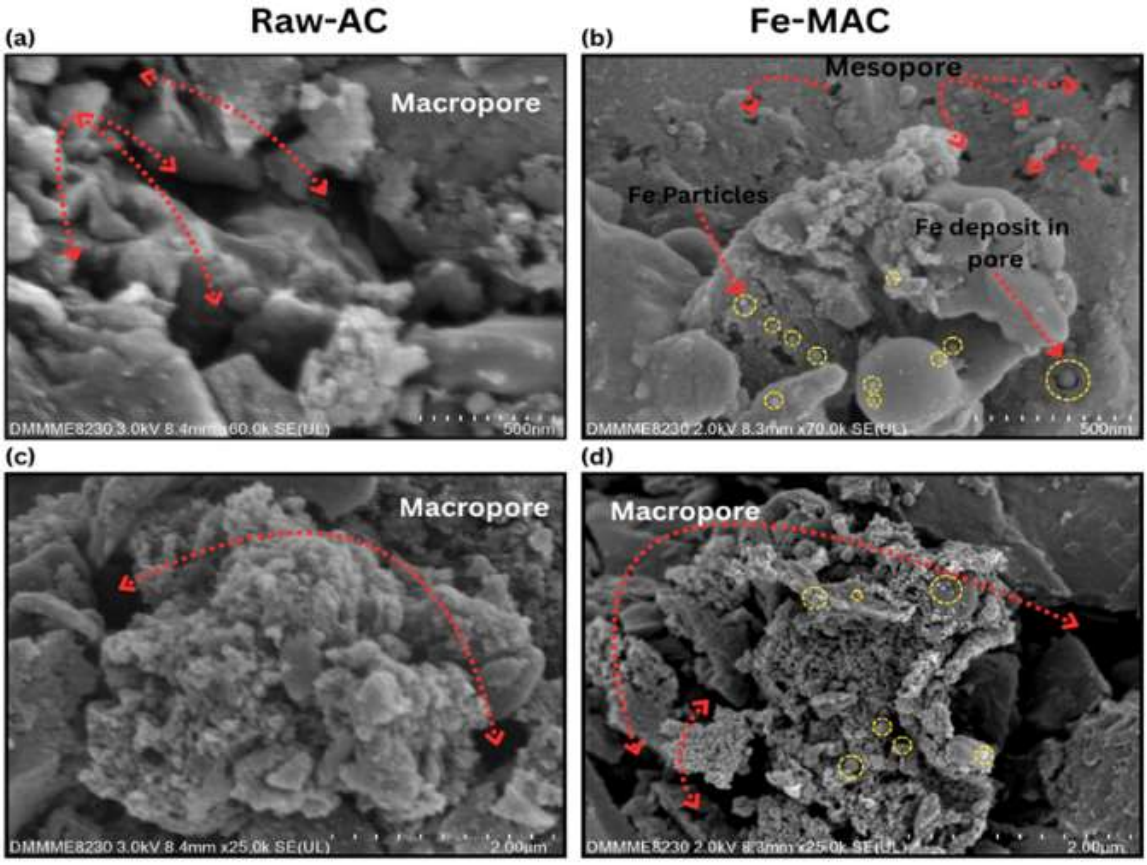

Figure 4: Surface Morphology of Activated Carbon Before and After Modification

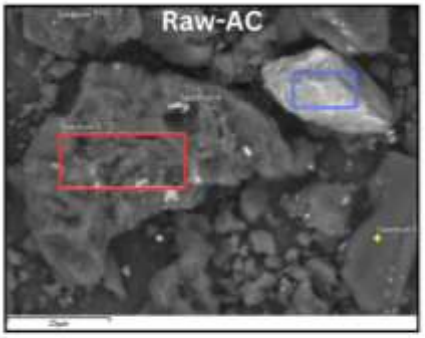

Element	Oxide	Oxide % Spectrum 1	Spectrum 2	Spectrum 3
C	CO2	97.96	83.41	99.39
Mg	MgO	0.04		-
Al	Al2O3	0.68	1.12	0.22
Si	SiO2	0.6	15.01	0.17
S	SO3	0.68	0.16	0.21
K	K2O	0.03	0.09	-
Fe	FeO		0.21	-

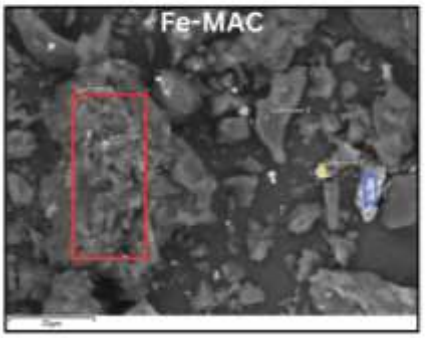

Element	Oxide	Oxide % Spectrum 6	Spectrum 7	Spectrum 8
C	CO2	97.32	80.68	89.48
Na	Na2O	-	0.06	
Mg	MgO	0.06	0.24	0.11
Al	Al2O3	0.92	5.43	3.16
Si	SiO2	0.72	11.22	3.9
S	SO3	0.56	0.38	0.43
Ca	CaO			1.1
K	K2O	0.03	0.82	0.1
Ti	TiO2	0.04	-	0.1
Fe	FeO	0.29	1.13	1.61

Figure 5: Comparison of Oxide composition of Raw-AC and Fe-MAC based on EDX Analysis

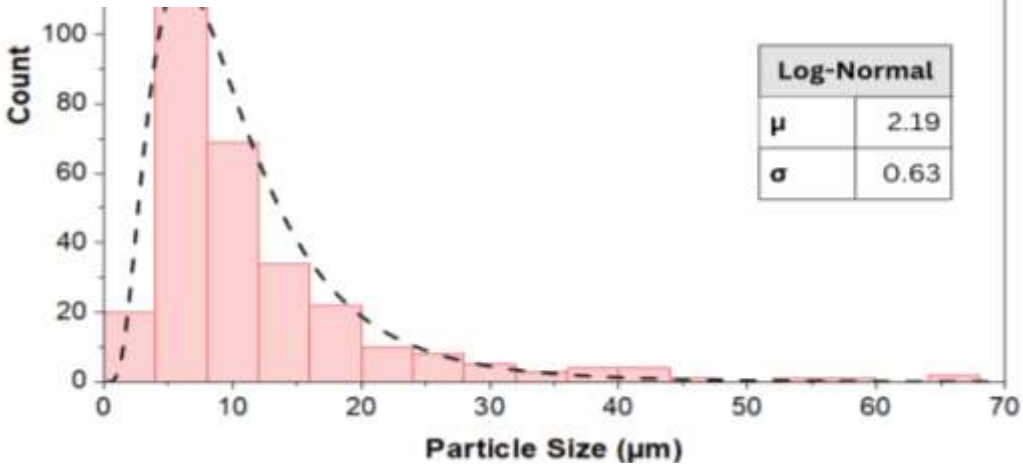

Figure 6: Particle Size Distribution of Activated Carbon

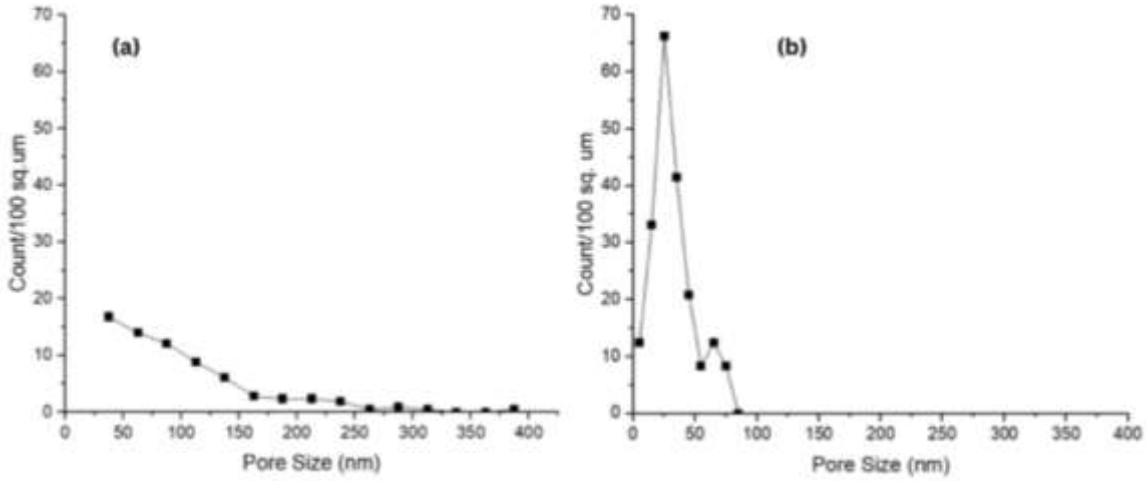

Figure 7: Pore Size Distribution of Activated Carbon Before (a) and After (b) Modification

3.2.2 Zeta Potential

The zeta potential before and after the modification of activated is shown in Figure 8. The point of zero charge (PZC) for AC and Fe-MAC was 3.12 and 4.29 respectively. The surface charge of Fe-MAC is positive when the solution pH is below 4.29 and becomes negative at pH values above this. This shift of zeta potential to the right resulting to more positive surface charge region due to iron impregnation was also observed in the studies of Kalaruban et al. (2019b) and Arcibar-Orozco et al. (2014b).

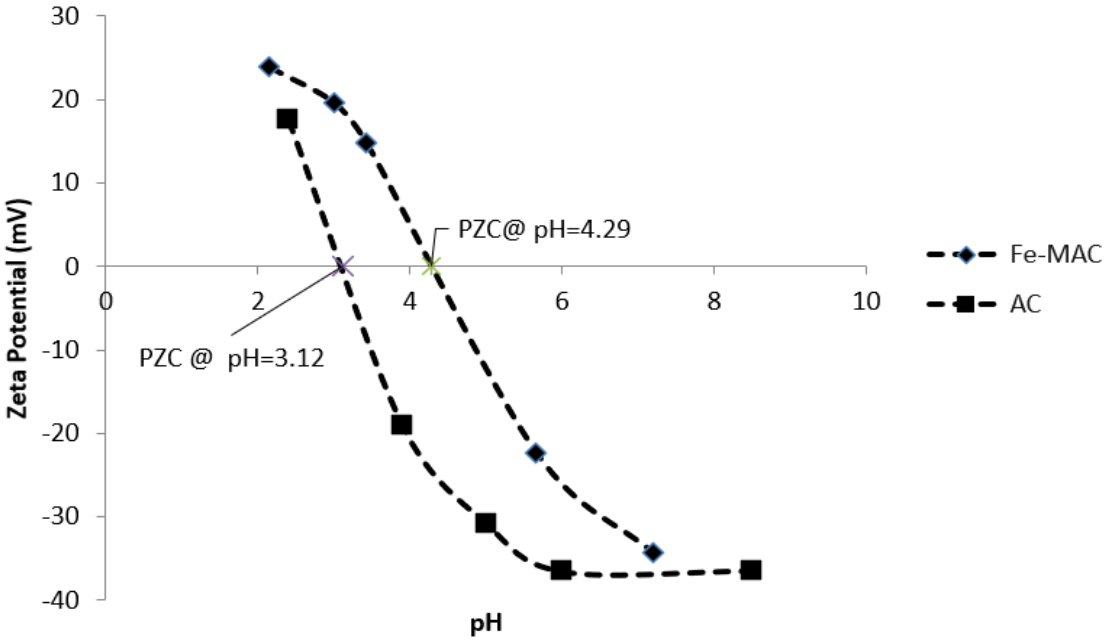

Figure 8: Zeta Potential of Activated Carbon Before and After the Modification

3.3 Batch Adsorption Results

The adsorption of arsenic on Fe-MAC was successful as suggested by the significant decrease of arsenic in the treated mine-wastewater with a maximum removal of 99% at initial arsenic concentration of 13.34 ppm, pH 9, and 8 g/L adsorbent dosage. The SEM image and elemental mapping of Fe-MAC after adsorption (Figure 10 and 11) provided evidence of arsenic being adsorbed onto the surface of the activated carbon. Distinct changes in the surface morphology were evident on Fe-MAC before and after the adsorption. The surface of the Fe-MAC before adsorption (Figure 10-a) appears clean and the pores are open and clear, while after adsorption (Figure 10-b), the pores are either partially or totally blocked indicating the presence of adsorbed arsenic and other elements. The EDX result in Figure 9 shows the elemental distribution of arsenic and iron on the surface of Fe-MAC. In Figure 9 (a), it can be observed that the arsenic is present and distributed throughout the surface of Fe-MAC. In addition, it is noticeable that, majority of the arsenic is distributed on the surface of the AC the same as the distribution of the iron (Figure 9-a and b). However, there is a certain part wherein no arsenic was adsorbed as highlighted by the red dashed line in Figure 9-c. Other elements are also adsorbed on the surface of the Fe-MAC. This reduced the available sites for adsorption of arsenic. Table 2 shows the concentrations of arsenic, and other elements on the Fe-MAC after the adsorption which supports the adsorption of arsenic and other metals.

Element	Wt%
C	78.89
O	8.78
Al	9.41
Si	0.84
S	0.95
Cl	0.09
K	0.1
Ti	0.14
Fe	0.79
As	0.01

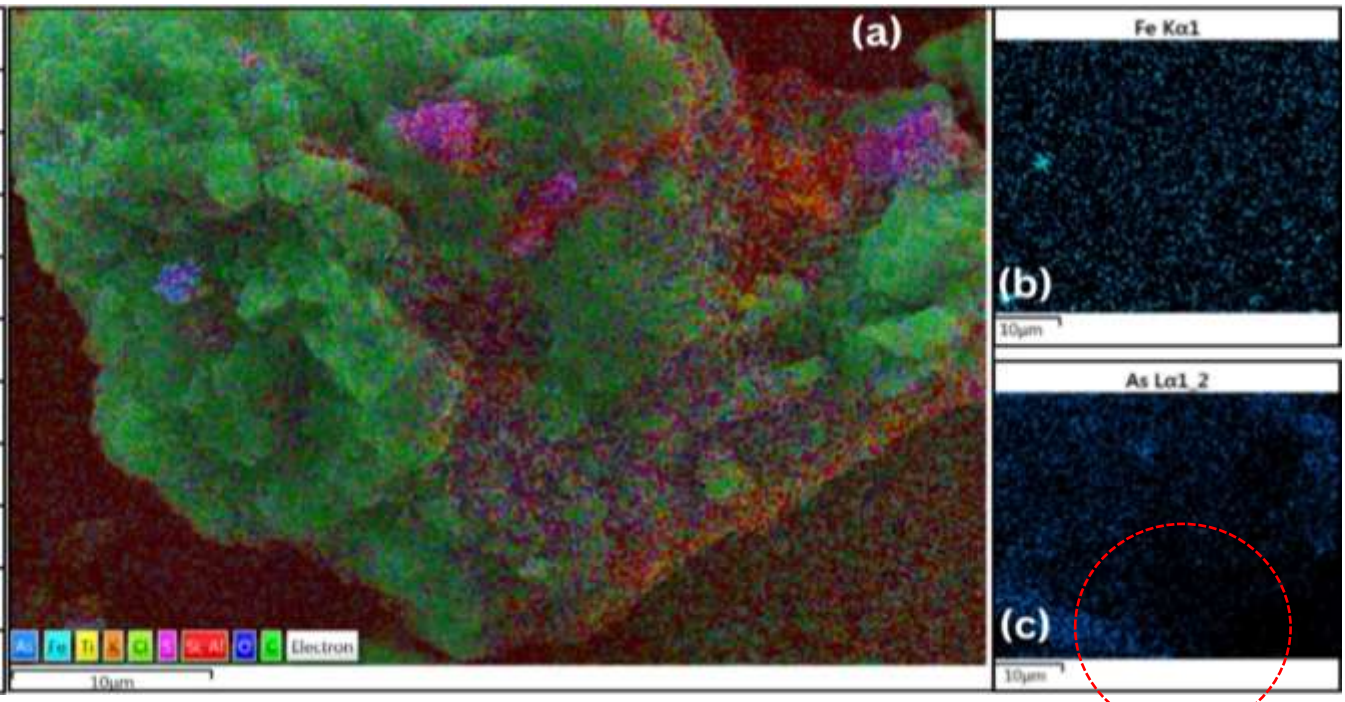

Figure 10: EDX Image and Elemental Mapping (a), distribution of iron (b), and arsenic (c) of Fe-MAC after the Adsorption

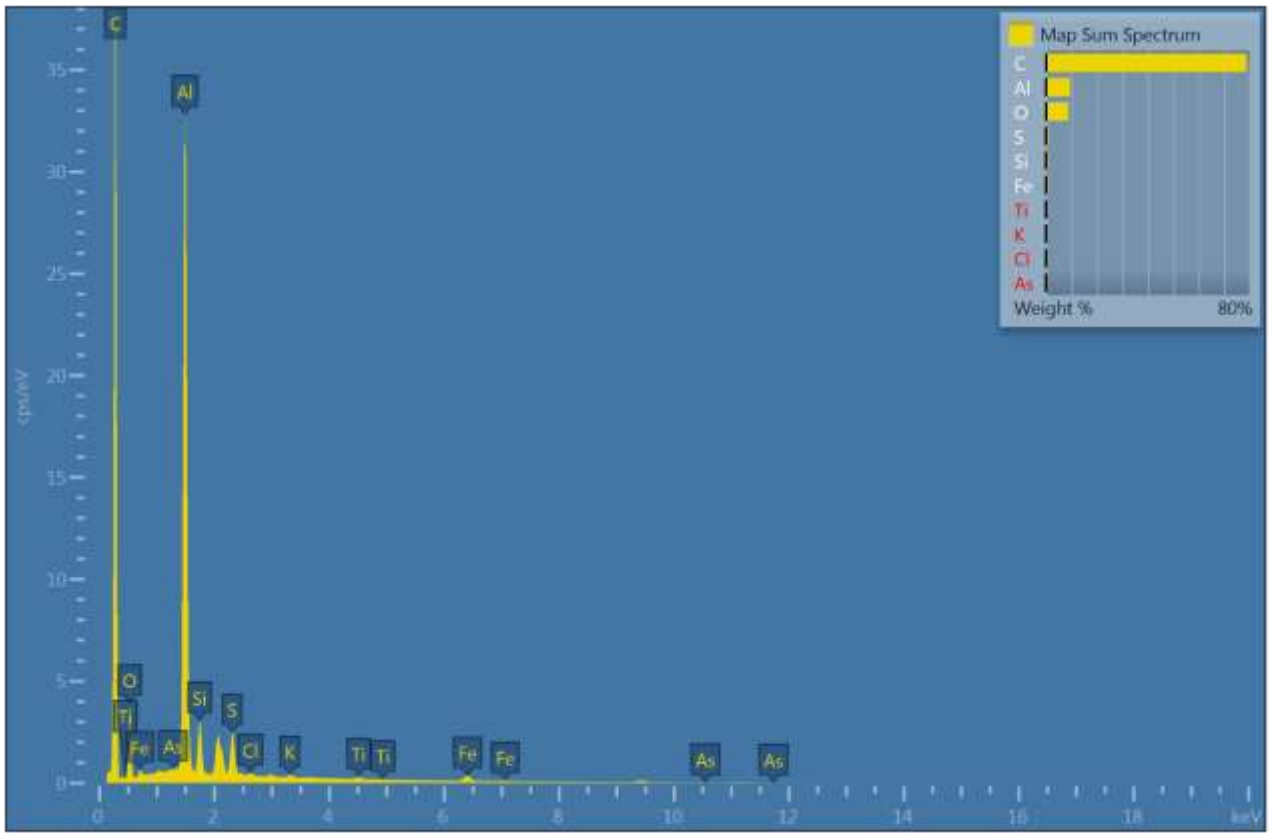

Figure 9: Elemental Mapping of Activated Carbon after Adsorption

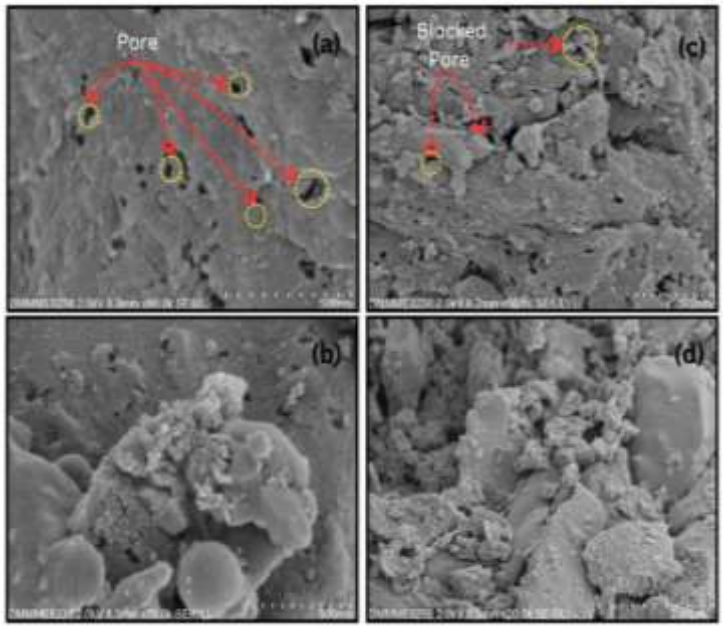

Fi

Table 2: XRF Analysis of Fe-MAC after Adsorption

Element	Concentration (ppm)
As	4039
Cu	8.9
Ni	8.7

3.3.1 Effect of Initial pH of Mine Wastewater

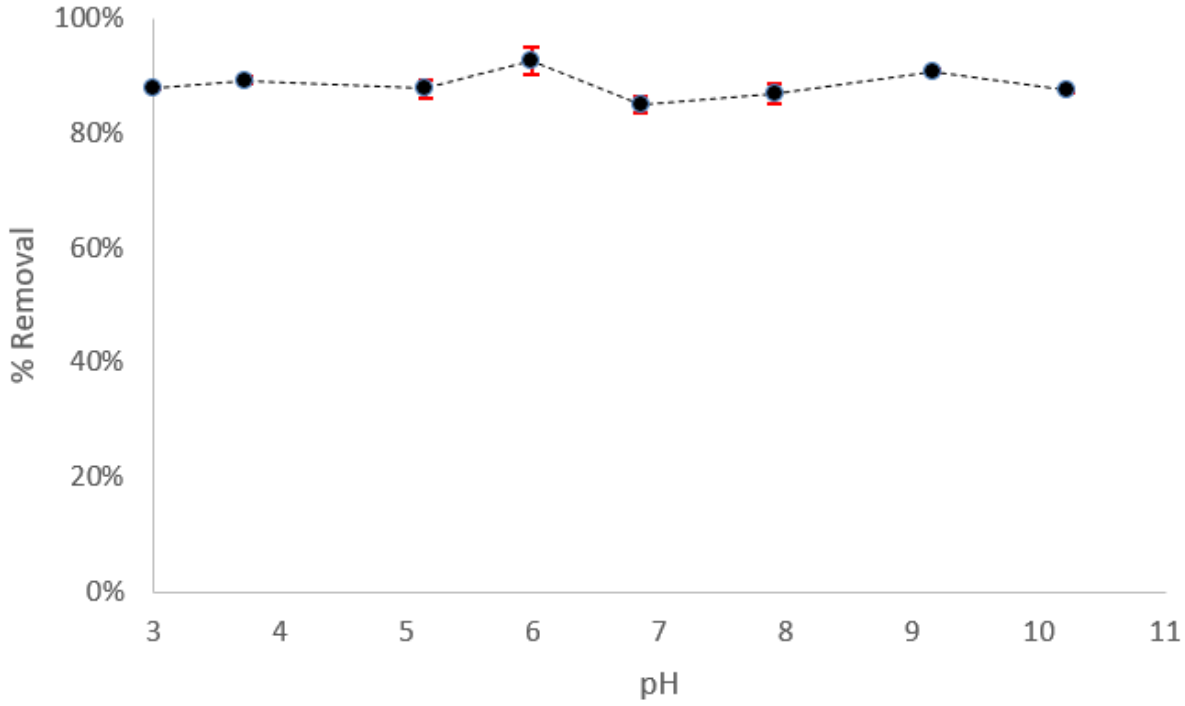

Figure 12: Effect of pH

The effect of initial pH of the mine wastewater was determined as it is crucial factor affecting in any adsorption. Results showed that significant removal was observed for all pH. The mine wastewater with initial pH 6.85 yielded the lowest arsenic removal of 84% followed by pH 8 with 85% removal. The highest arsenic removal of 95% was obtained from the mine-wastewater with an initial pH 6 as shown in Figure 12. It can be seen in Figure 13 that the final pH of the mine-wastewater after the adsorption was in the range of 5-8 regardless of the initial pH. Similar behavior was reported by Ha et al. (2021), Kalaruban et al. (2019), Liu et al. (2012) and Yang et al. (2009) where the final pH of the treated wastewater was close to neutral regardless of the initial pH. The authors attributed this to the residual alkalinity of iron impregnated activated carbon. In this study, the behavior of having a near neutral final pH after the adsorption across initial pHs could have been influenced by the alkalinity of the Fe-MAC and the acidic reaction during the adsorption of

certain elements onto the Fe-MAC. This is further discussed in the succeeding sections. However, it is suggested that a further study be conducted on the behavior or performance of Fe-MAC when the pH changes during the adsorption.

In the succeeding tests, the initial pH ≈9 was selected as the operational initial pH of the mine-wastewater despite having a slightly lower arsenic removal (91%) than the highest observed removal of 95% at pH 6. This is in consideration of the large amount of acid required to lower the pH of the mine-wastewater if applied in a large-scale operation. In terms of adsorption mechanism, the result of the effect pH does not support the electrostatic attraction as adsorption mechanism due to charge repulsion. At acidic pH, As (III) and As (V) exist majority as $H_3AsO_3^o$ and $H_2AsO_4^-$ respectively. And at pH 9.2, As (III) $H_3AsO_3^o$ starts to deprotonate to $H_2AsO_3^-$ while for As (V) the $H_2AsO_4^-$ starts to deprotonate at pH 7 $H_2AsO_4^{2-}$ (Smedley & Kinniburgh, 2002b). At the operating pH of 9, the Fe-MAC is negatively charge as seen in Figure 5, while and the arsenic species exist are $H_3AsO_3^o$ and $H_2AsO_4^{2-}$ for As (III) and As (V) respectively (Smedley & Kinniburgh, 2002b).

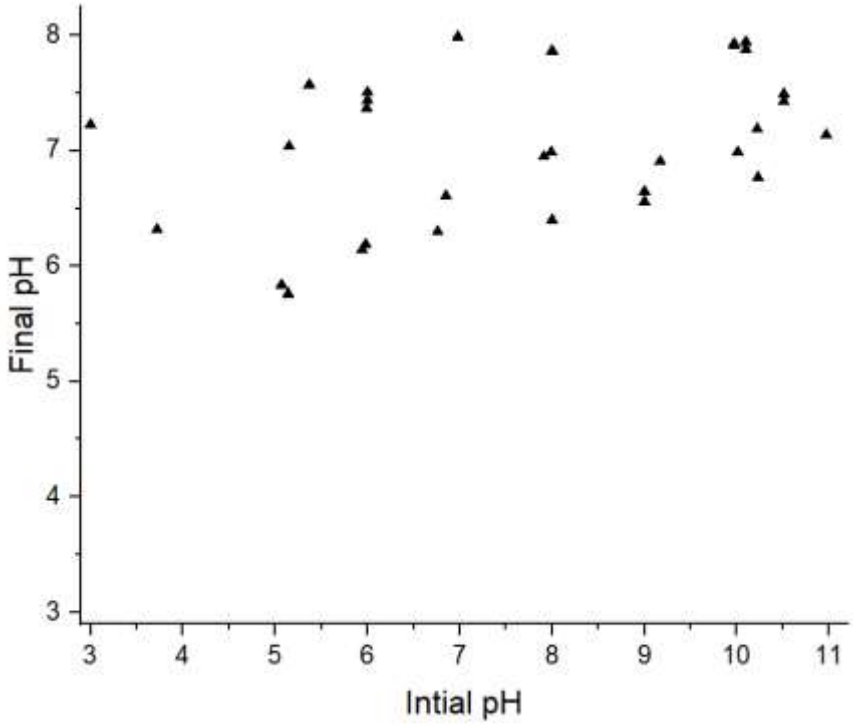

Figure 13: pH Shift Before and After the Adsorption

3.3.2 Effect of Adsorbent Dosage

The effect of adsorbent dosage on the removal of arsenic and adsorption capacity of the Fe-MAC was investigated. The Results is shown in Figure 14. It is apparent that increasing the adsorbent dosage increases the removal. This is due to more adsorption sites available as the adsorbent dosage was increased. In contrast, the adsorption capacity decreases with increasing adsorbent dosage. Note that the initial concentration of arsenic in the mine-wastewater and contact time were set constant. Hence, the higher adsorption dosage means more adsorption sites and less likely that these sites will be saturated quickly. With lower adsorbent dosage, the adsorption sites were limited leading to saturation with arsenic and other ions. The adsorbent has achieved or almost achieved its adsorption capacity, hence the high adsorption capacity. At higher adsorbent dosage, lower adsorption capacity indicates more remaining adsorption sites unoccupied. The adsorption capacity is not achieved due to more available adsorption sites than the particles to be adsorbed.

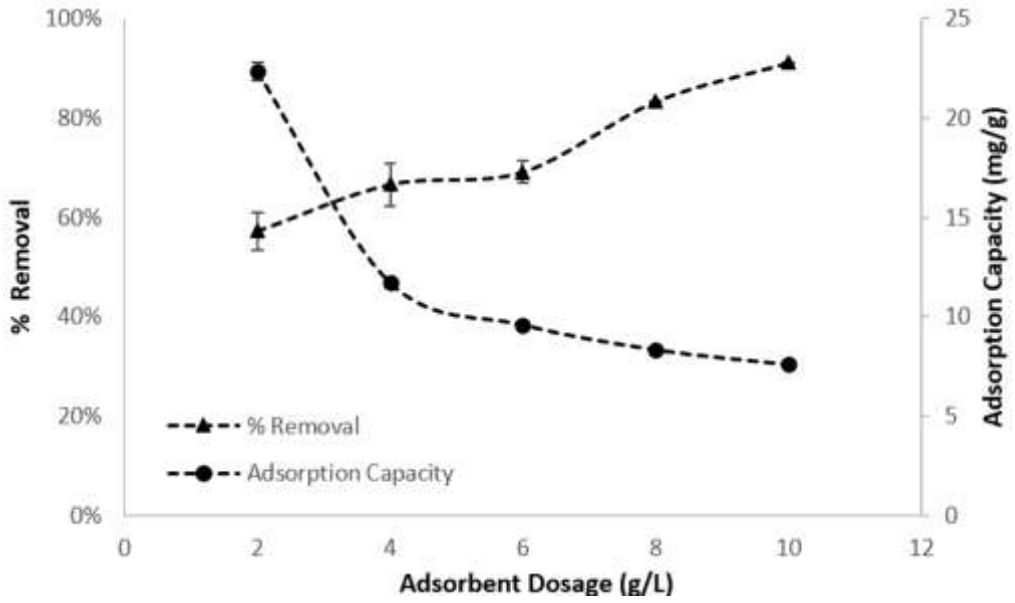

Figure 14: Effect of Adsorbent Dosage

3.4 Kinetic Modelling

The adsorption data is well fitted in pseudo-second order (PSO) model with R^2 of 0.997. The predicted maximum adsorption capacity of pseudo-second order was closer to the actual. On the other hand, the pseudo first order has an R^2 of 0.84 and was not able to predict the adsorption capacity (Table 3). This suggests that the pseudo-second order is the better predictive model of the adsorption, indicating that the rate-limiting step may involve chemisorption. The Weber-Morris model depicted in Figure 13 does not result in a good-fit, hence does not support an intraparticle diffusion as rate-limiting step.

Table 3: Parameter Values of Batch Adsorption for Kinetic Modelling

Pseudo-First Order	qe	mg/g	2.314
	k1	h^{-1}	0.24
		R^2	0.84
Pseudo-Second Order	qe	mg/g	4.35
	k2	h^{-1}	0.3
		R^2	0.997
Weber and Morris	k2	$mg/g/h^{1/2}$	0.659
		R^2	0.742

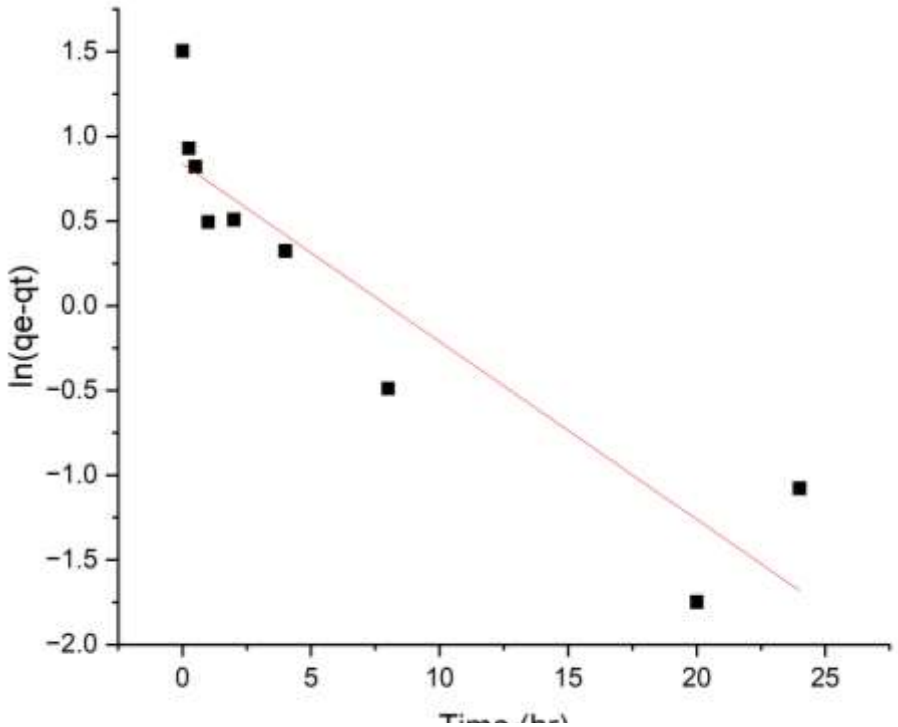

Figure 11: Kinetic Modelling of Arsenic Adsorption Data Fitted Using Pseudo-First Order Model

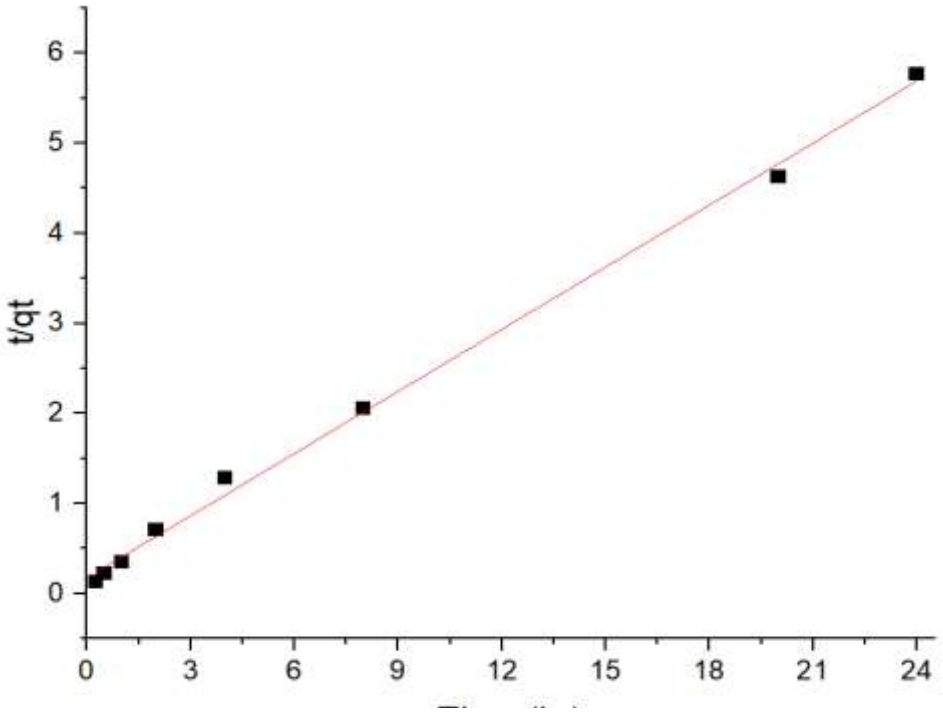

Figure 12: Kinetic Modelling of Arsenic Adsorption Data Fitted Using Pseudo-Second-Order Model

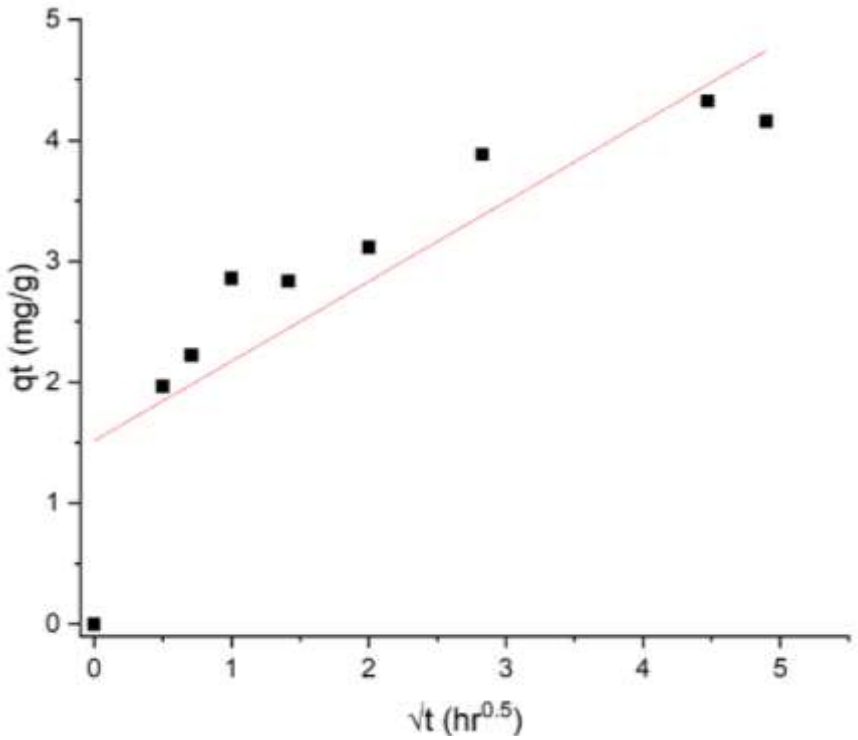

Figure 13: Kinetic Modelling of Arsenic Adsorption Data Fitted Using Weber-Morris Model

The adsorption behavior of arsenic and other metals from mine-wastewater over time revealed distinct trends that provide insights into the interaction between arsenic species, competing ions such as copper and nickel, and the Fe-MAC. At the beginning, the adsorption of arsenic on iron impregnated activated carbon was rapid. In the first hour, 53% of the arsenic was already removed and then a transition rate was observed reaching only 58% for the next two hours until the maximum adsorption was reached. This could be due to other metals also being adsorbed such as copper and nickel. These metals occupy some adsorption sites reducing the available sites for arsenic. Hence, for the succeeding hour, the arsenic species took more time to find available adsorption sites. For Fe, alternating increase and decrease in concentration were observed until a peak at 4 h, followed by a sharp drop at 8 h and a gradual decline up to 24 h. This trend suggests that the Fe was possibly initially leached from the Fe-MAC and re-adsorbed then re-desorbed alternately. Note that the leaching of iron from Fe-MAC did not affect the arsenic adsorption suggesting instability of iron on the Fe-MAC when contacted with high ionic strength solution at dynamic pH.

For Cu, 82 % removal was already achieved at only 15 minutes contact time and decreased to 64% at 4 hours contact time. It reached 80% removal at equilibrium indicating that the Cu has underwent adsorption-desorption. Studies showed that, copper adsorption on iron impregnated activated carbon is typically influenced by electrostatic attraction, surface complexation, ion exchange or the combination of the three mechanisms (Shan et al., 2020; Peacock & Sherman, 2004; J.-K. Yang et al., 2009). At low pH (2-6.5) copper occurs mainly as cation (Cu^{2+}) whereas above pH 7 it exists primarily as $Cu_2(OH)_2^{2+}$ as a result of hydrolysis (Peacock & Sherman, 2004). Generally, copper adsorption using Fe-AC favors high pH (≈ >5.5) where surface complexation with impregnated iron occurs according to Eq.1. (J.-K. Yang et al., 2009). The complexation generated H^+ which could have contributed to the lowering of pH of the of the mine-wastewater after the adsorption.

$$Fe-OH + Cu^{2+} \rightarrow Fe-O-Cu^{+} + H^{+}$$

For Ni, rapid adsorption occurred within the first 30 minutes, achieving 94% removal. This was followed by a gradual decrease of removal up to 2 hours (Figure 14) suggesting possible desorption of the metal ions. Subsequently, a complete removal was achieved at equilibrium time. Research studies showed that the adsorption of nickel increases at increasing pH. This is attributed to the competition of H^+ and the nickel at lower pH (Abd El-Magied et al., 2018). Below pH 8, nickel exists as Ni^{2+} while Ni $(OH)_2^0$ and Ni $(OH)_3^{-1}$ exist at higher pH. The rapid removal at first 30 minutes is likely due to the favorable electrostatic attraction of the negatively charged Fe-MAC and the positively charged Ni^{2+} and Ni $(OH)^+$ at initial pH of 9.

Adsorption favored the removal of nickel (Ni^{2+}) over copper (Cu^{2+}) achieving 100% removal at 20 hours contact time. This result could be due to the nickel having smaller ionic radius of 0.69 Å as compared to 0.72 Å of copper which

allows it to diffuse into the pores of AC (Khelifi et al., 2022). The higher removal of copper at the beginning of contact could be due to the stronger affinity of copper than nickel (Zheng et al., 2021). Furthermore, the slower removal rate of arsenic at initial stages of adsorption as compared to copper and nickel could be attributed to its relatively large ionic radius of 1.33 Å. Other metals such as Na, Cr, and Ca were also detected (Table 3). Their presence could have may have influenced the adsorption behavior of arsenic and other co-existing metals.

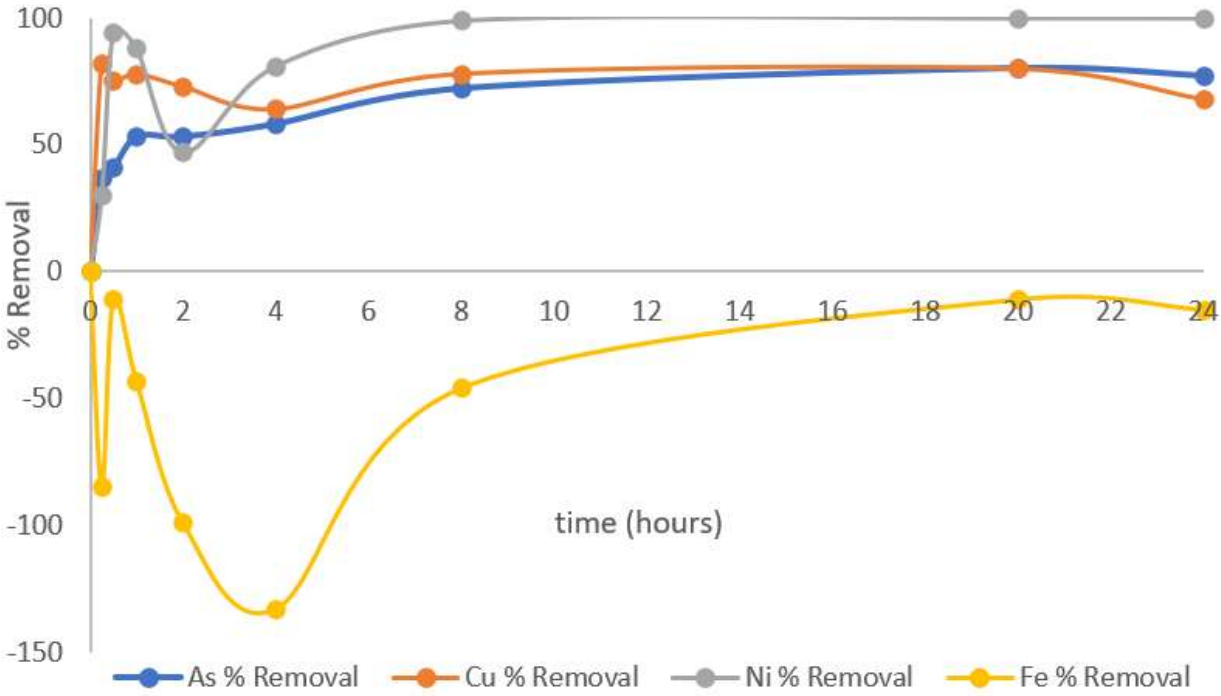

Figure 14: Removal Behavior of Arsenic and Competing Metals as a Function of Contact Time

4. SUMMARY AND CONCLUSION

The growing reliance of the mining industry to arsenic bearing ore may lead to higher risk of arsenic exposure and contamination. With this, sustainable treatment method is necessary to protect the environment and the people from risk of arsenic contamination. This study focused on the removal of arsenic from mine wastewater using a modified activated carbon. The modification involved impregnating the activated carbon with iron.

The batch adsorption experiments results showed that the iron impregnated activated carbon (Fe-MAC) is effective in removing arsenic and other ions from mine-wastewater achieving a maximum of 99% As removal efficiency. The optimum pH of the adsorption is 9. The pH after adsorption converged to near neutral regardless of the initial pH. The optimum adsorbent dosage is 10 g/L. The removal increases with increasing adsorbent dosage due to more adsorption sites at higher dosage, while the adsorption capacity decreases with increasing adsorbent dosage due to unutilized adsorption sites at higher dosage.

The adsorption data is well fitted on pseudo-second order suggesting that the rate-limiting step may involve chemisorption. The predicted adsorption equilibrium is 20 hours. Other metals were also adsorbed such as copper and nickel. The adsorption of arsenic was rapid initially at first 3 hours along with copper and nickel followed by slow rate adsorption until adsorption equilibrium. This suggests that arsenic required more time to access available adsorption sites due to competition from other metal ions. Moreover, iron was initially leached from the activated carbon and subsequently re-adsorbed, indicating its instability under the conditions of mine-wastewater.

The results of this research showed that the iron impregnated activated carbon (Fe-MAC) successfully remove the arsenic from the mine wastewater. Specifically, the following conclusion can be drawn:

a. The iron impregnation successfully enhanced the surface properties of activated carbon achieving maximum 99% arsenic removal, indicating high affinity to arsenic.
b. The iron impregnation shifted the point zero charge of AC, resulting to widened positive surface charge region.
c. The adsorption performance was found to be weakly influenced by the pH due to the convergence to near neutral final pH regardless of the initial pH. In contrast, increasing the adsorbent dosage significantly enhanced the removal efficiency, with maximum removal achieved at 10 g/L.
d. The kinetic analysis showed that the arsenic

adsorption followed pseudo-second order model suggesting that the rate-limiting step may involve chemisorption.

Due to resources limitation, arsenic speciation analysis was not established in this study, which could provide deeper insights into the adsorption mechanisms.

REFERENCES

1. Abd El-Magied, M. O., Hassan ,Ali M. A., Gad ,Hamdi M. H., Mohammaden ,Tarek F., & and Youssef, M. A. M. (2018). Removal of nickel (II) ions from aqueous solutions using modified activated carbon: A kinetic and equilibrium study. *Journal of Dispersion Science and Technology*, *39*(6), 862–873.
2. Ahmad, S. A., Khan, M. H., & Haque, M. (2018). Arsenic contamination in groundwater in Bangladesh: Implications and challenges for healthcare policy. *Risk Management and Healthcare Policy*, *11*, 251–261.
3. Alarcón-Herrera, M. T., Bundschuh, J., Nath, B., Nicolli, H. B., Gutierrez, M., Reyes-Gomez, V. M., Nuñez, D., Martín-Dominguez, I. R., & Sracek, O. (2013). Co-occurrence of arsenic and fluoride in groundwater of semi-arid regions in Latin America: Genesis, mobility and remediation. *Journal of Hazardous Materials*, *262*, 960–969.
4. Arcibar-Orozco, J. A., Josue, D.-B., Rios-Hurtado, J. C., & Rangel-Mendez, J. R. (2014). Influence of iron content, surface area and charge distribution in the arsenic removal by activated carbons. *Chemical Engineering Journal*, *249*, 201–209.
5. CDC. (2024, November 7). *Substance Priority List*. Agency for Toxic Substances and Disease Registry.
6. Garelick, H., Jones, H., Dybowska, A., & Valsami-Jones, E. (2009). Arsenic pollution sources. *Rev Environ Contam Toxicol*, *97*, 17–60.
7. Ha, H. T., Phong, P. T., & Minh, T. D. (2021). Synthesis of Iron Oxide Nanoparticle Functionalized Activated Carbon and Its Applications in Arsenic Adsorption. *Journal of Analytical Methods in Chemistry*, *2021*, 6668490.
8. Ho, Y. S., & McKay, G. (1999). Pseudo-second order model for sorption processes. *Process Biochemistry*, *34*(5), 451–465.
9. Kalaruban, M., Loganathan, P., Nguyen, T. V., Nur, T., Hasan Johir, M. A., Nguyen, T. H., Trinh, M. V., & Vigneswaran, S. (2019). Iron-impregnated granular activated carbon for arsenic removal: Application to practical column filters. *Journal of Environmental Management*, *239*, 235–243.
10. Karmacharya, M. S., Gupta, V. K., Tyagi, I., Agarwal, S., & Jha, V. K. (2016). Removal of As(III) and As(V) using rubber tire derived activated carbon modified with alumina composite. *Journal of Molecular Liquids*, *216*, 836–844.
11. Kobya, M., Soltani, R. D. C., Omwene, P. I., & Khataee, A. (2020). A review on decontamination of arsenic-contained water by electrocoagulation: Reactor configurations and operating cost along with removal mechanisms. *Environmental Technology & Innovation*, *17*, 100519.
12. *Lagergren, S. (1898) Zur theorie der sogenannten adsorption geloster stoffe, Kungliga Svenska Vetenskapsakademiens. Handlingar, 24, 1-39. - References—Scientific Research Publishing*. (n.d.).
13. Liang, C.-P., Wang, S.-W., Kao, Y.-H., & Chen, J.-S. (2016). Health risk assessment of groundwater arsenic pollution in southern Taiwan. *Environmental Geochemistry and Health*, *38*(6), 1271–1281.
14. Liu, X., Ao, H., Xiong, X., Xiao, J., & Liu, J. (2012). Arsenic Removal from Water by Iron-Modified Bamboo Charcoal. *Water, Air, & Soil Pollution*, *223*(3), 1033–1044.
15. Method 3114, Standard Methods Committee, 2009. (2017). 3114 arsenic and selenium by hydride generation atomic absorption spectrometry. In *Standard Methods For the Examination of Water and Wastewater*. American Public Health Association.
16. Pawar, R. R., Lalhmunsiama, Kim, M., Kim, J.-G., Hong, S.-M., Sawant, S. Y., & Lee, S. M. (2018). Efficient removal of hazardous lead, cadmium, and arsenic from aqueous environment by iron oxide modified clay-activated carbon composite beads. *Applied Clay Science*, *162*, 339–350.
17. Peacock, C. L., & Sherman, D. M. (2004). Copper(II) sorption onto goethite, hematite and lepidocrocite: A surface complexation model based on ab initio molecular geometries and EXAFS spectroscopy1. *Geochimica et Cosmochimica Acta*, *68*(12), 2623–2637.
18. Phyu, K. P., Win, K. K. N., Hlaing, M. M., Zaw, K. M., Han, T. T., Marlar, M., Aung, M. N., Zin, P. W., Naing, A., Konishi, A., Morita, Y., & Htun, Z. T. (2020). Assessment and treatment of arsenic contaminated tube well water from selected areas in Kyaunggon Township, Ayeyarwady Region, Myanmar. *IOP Conference Series: Earth and Environmental Science*, *496*(1), 012009.
19. Podgorski, J., & Berg, M. (2020). Global threat of arsenic in groundwater. *Science (New York, N.Y.)*, *368*(6493), 845–850.
20. Shan, R., Shi, Y., Gu, J., Wang, Y., & Yuan, H. (2020). Single and competitive adsorption affinity of

heavy metals toward peanut shell-derived biochar and its mechanisms in aqueous systems. *Chinese Journal of Chemical Engineering*, *28*(5), 1375–1383.

21. Siddiqui, S. I., & Chaudhry, S. A. (2017). Iron oxide and its modified forms as an adsorbent for arsenic removal: A comprehensive recent advancement. *Process Safety and Environmental Protection*, *111*, 592–626.
22. Sigrist, M. E., Brusa, L., Beldomenico, H. R., Dosso, L., Tsendra, O. M., González, M. B., Pieck, C. L., & Vera, C. R. (2014). Influence of the iron content on the arsenic adsorption capacity of Fe/GAC adsorbents. *Journal of Environmental Chemical Engineering*, *2*(2), 927–934. https://doi.org/10.1016/j.jece.2014.02.013
23. Smedley, P. L., & Kinniburgh, D. G. (2002). A review of the source, behaviour and distribution of arsenic in natural waters. *Applied Geochemistry*, *17*(5), 517–568.
24. Verma, L., & Singh, J. (2019). Synthesis of novel biochar from waste plant litter biomass for the removal of Arsenic (III and V) from aqueous solution: A mechanism characterization, kinetics and thermodynamics. *Journal of Environmental Management*, *248*, 109235.
25. Waseem, U. (n.d.). Scanning Electron Microscopy: A Comprehensive Guide. Retrieved June 17, 2025, from https://www.wevolver.com/article/scanning-electron-microscopy-a-comprehensive-guide, https://www.wevolver.com/article/scanning-electron-microscopy-a-comprehensive-guide
26. Weber, W. J., & Morris, J. C. (1963). Kinetics of Adsorption on Carbon from Solution. *Journal of the Sanitary Engineering Division*, *89*(2), 31–59. https://doi.org/10.1061/JSEDAI.0000430
27. Weerasundara, L., Ok, Y.-S., & Bundschuh, J. (2021). Selective removal of arsenic in water: A critical review. *Environmental Pollution*, *268*, 115668.
28. Yang, J.-K., Park, H.-J., Lee, H.-D., & Lee, S.-M. (2009). Removal of Cu(II) by activated carbon impregnated with iron(III). *Colloids and Surfaces A: Physicochemical and Engineering Aspects*, *337*(1), 154–158.
29. Yang, R., Su, Y., Aubrecht, K. B., Wang, X., Ma, H., Grubbs, R. B., Hsiao, B. S., & Chu, B. (2015). Thiol-functionalized chitin nanofibers for As (III) adsorption. *Polymer*, *60*, 9–17.
30. Zakhar, R., Derco, J., & Čacho, F. (2018a). An overview of main arsenic removal technologies. *Acta Chimica Slovaca*, *11*(2), 107–113.
31. Zakhar, R., Derco, J., & Čacho, F. (2018b). An overview of main arsenic removal technologies. *Acta Chimica Slovaca*, *11*(2), 107–113.
32. Zhang, Q. L., Lin, Y. C., Chen, X., & Gao, N. Y. (2007). A method for preparing ferric activated carbon composites adsorbents to remove arsenic from drinking water. *Journal of Hazardous Materials*, *148*(3), 671–678. https://doi.org/10.1016/j.jhazmat.2007.03.026
33. Zhuang, F., Huang, J., Li, H., Peng, X., Xia, L., Zhou, L., Zhang, T., Liu, Z., He, Q., Luo, F., Yin, H., & Meng, D. (2023). Biogeochemical behavior and pollution control of arsenic in mining areas: A review. *Frontiers in Microbiology*, *14*.
34. Zhuang, F., Huang, J., Li, H., Peng, X., Xia, L., Zhou, L., Zhang, T., Liu, Z., He, Q., Luo, F., Yin, H., & Meng, D. (2023). Biogeochemical behavior and pollution control of arsenic in mining areas: A review. Frontiers in Microbiology, 14.